Chapter 2
OFDM Based Wireless Communications Systems

2.1 OFDM Technology

To eliminate the Inter-Symbol Interference (ISI) due to multipath, traditional time-domain equalization schemes [1–3] in the literature require complex implementation, and thus are practically impossible. Due to technological development, the digital implementation of the pair of Fast Fourier Transform (FFT) and Inverse Fast Fourier Transform (IFFT) becomes simple and practically possible. OFDM technology, proposed in 1960 [4], is attractive for simplifying the equalization process at the receiver for frequency selective fading channels [5]. So far, OFDM has been chosen for the wireless local area networks IEEE 802.11 standards [6], and has been adopted by LTE-Advanced [7, 8]. Also, it has been selected as a strong candidate for the WiGig [9, 10] and the Fifth Generation (5G) wireless communication [11, 12] in the future, respectively.

2.1.1 Principle of OFDM

Different from the single carrier modulation which has a relatively low data rate, the multi-carrier modulation [5] is employed to support high data rates in OFDM technology. In OFDM, a frequency band is divided into a number of closely spaced spectrums. Thanks to the orthogonal property of subcarriers, the center frequency of one subcarrier can coincide with the spectral zeros of all other subcarriers, leading to no interference between subcarriers. To guarantee the orthogonality between subcarriers, a small spacing between subcarriers is used in OFDM systems, while a bigger spectral width between parallel channels is used to avoid the interference

Y. Jiang et al., *Semi-Blind Carrier Frequency Offset Estimation and Channel Equalization*, SpringerBriefs in Electrical and Computer Engineering,
DOI 10.1007/978-3-319-24984-1_2

in traditional Frequency Division Multiplexing (FDM) systems [13, 14]. Therefore, OFDM systems can achieve higher spectral efficiency than FDM systems.

In order to combat frequency selective fading, a high-rate transmit stream is divided into a large number of low-rate substreams. Consequently, the symbol period on each subcarrier is prolonged, and the signal bandwidth becomes shorter in comparison to the channel coherence bandwidth. Assuming that the channel variation is slow, the symbol duration T_s can satisfy

$$\sigma_{\text{rms}} < NT_s < T_c, \tag{2.1}$$

where N is the number of subcarriers, σ_{rms} and T_c are the Root Mean Square (RMS) delay spread of the channel and the channel coherent time, respectively.

Therefore, the frequency selective fading channel can be divided into a number of frequency flat fading channels. As the ISI is avoided, OFDM systems require equalization with lower complexity than that employed in traditional methods as in [1–3].

2.1.2 CFO

Although OFDM can combat frequency selective fading, there are some drawbacks to OFDM systems. One of drawbacks is the CFO. Generally, the signal is converted up to a passband by a carrier at the transmitter, and converted down to the baseband by the same carrier at the receiver, via LOs. This type of CFO is caused by the unavoidable difference of LOs between transmitter and receiver. The CFO destroys the orthogonality between OFDM subcarriers, and results in the ICI. As a result, the CFO can incur a significant degradation in BER performance.

f_r and f_t are defined as the carrier frequencies at the receiver and transmitter, respectively. The normalized CFO ϕ can be written as

$$\phi = \frac{f_r - f_t}{\triangle f}, \tag{2.2}$$

where $\triangle f$ denotes the subcarrier spacing.

Define $\mathbf{s} = [s(0), s(1), \ldots, s(N-1)]^T$ as the transmitted signal vector. Considering the effect of CFO, the received signal vector $\mathbf{y}^{(\phi)} = [y^{(\phi)}(0), y^{(\phi)}(1), \ldots, y^{(\phi)}(N-1)]^T$ in the frequency domain for OFDM systems can be written as

$$\mathbf{y}^{(\phi)} = \mathbf{F}\boldsymbol{\Phi}^{(\phi)}\mathbf{F}^H\mathbf{H}\mathbf{s} + \mathbf{z}_f, \tag{2.3}$$

where $\mathbf{F}$ is an $N \times N$ Discrete Fourier Transform (DFT) matrix, with entry (a, b) given by $\mathbf{F}(a, b) = \frac{1}{\sqrt{N}} e^{\frac{-j2\pi ab}{N}}, (a, b = 0, \ldots, N-1)$, and $\mathbf{F}^H$ is an Inverse

Discrete Fourier Transform (IDFT) matrix, $\boldsymbol{\Phi}^{(\phi)} = \text{diag}\{[0, e^{\frac{j2\pi\phi}{N}}, \ldots, e^{\frac{j2\pi\phi(N-1)}{N}}]\}$ is the diagonal CFO matrix, with diag$\{\mathbf{x}\}$ denoting a diagonal matrix whose diagonal elements are entries of vector $\mathbf{x}$, $\mathbf{H} = \text{diag}\{[H(0), H(1), \ldots, H(N-1)]\}$ is the diagonal frequency-domain channel matrix, with $H(n)$ denoting the channel frequency response on the n-th subcarrier, and $\mathbf{z}_f$ is the $N \times 1$ Additive White Gaussian Noise (AWGN) vector.

Note that the CFO has a range of $[-0.5,\ 0.5)$ [15]. The ICI matrix caused by the CFO is written as $\mathbf{C}^{(\phi)} = \mathbf{F}\boldsymbol{\Phi}^{(\phi)}\mathbf{F}^H$. The ICI matrix $\mathbf{C}^{(\phi)}$ is circular, with each row equal to the previous one rotated by one element [16]. With the effect of the CFO, the received signal vector $\mathbf{y}^{(\phi)}$ can be written as

$$\mathbf{y}^{(\phi_f)} = \mathbf{C}^{(\phi)}\mathbf{H}\mathbf{s} + \mathbf{z}_f. \tag{2.4}$$

The frequency component on the n-th subcarrier is affected by the ICI from other $(N-1)$ subcarriers. In such a case, the orthogonality between subcarriers is destroyed by the CFO.

In a fast moving environment, the Doppler shift is determined by carrier frequency and velocity. This effect gives rise to time-varying channels in the time domain, and a frequency drift between subcarriers in the frequency domain. Thus, the orthogonality between subcarriers could not be maintained.

2.1.3 OFDMA

Recently, OFDMA, derived from OFDM, has attracted much research attention. It has been adopted by the Digital Video Broadcasting - Return Channel Terrestrial (DVB-RCT) [17], and the wireless local area networks IEEE 802.11 standards [6, 18].

Different from OFDM systems in which a single user occupies all subcarriers for the signal transmission, OFDMA systems allow multiple users to transmit symbols simultaneously using different orthogonal subcarriers. In OFDMA systems, a subset of subcarriers is assigned to each user, and the number of subcarriers for an individual user can be adaptively varied in each frame. Furthermore, OFDMA systems can provide a relatively lower PAPR than OFDM systems.

OFDMA has dynamic resource allocation, as it allows users to select their own subset of subcarriers according to channel conditions. Generally, there are three kinds of Carrier Assignment Scheme (CAS) available for users in OFDMA systems: subband CAS, interleaved CAS and generalized CAS, as shown in Fig. 2.1 [19].

- **Subband CAS**: several adjacent subcarriers are composed into a subblock to be allocated for an individual user.
- **Interleaved CAS**: the subcarriers of users are interleaved, and are uniformly spaced over the signal bandwidth at a distance from each other.

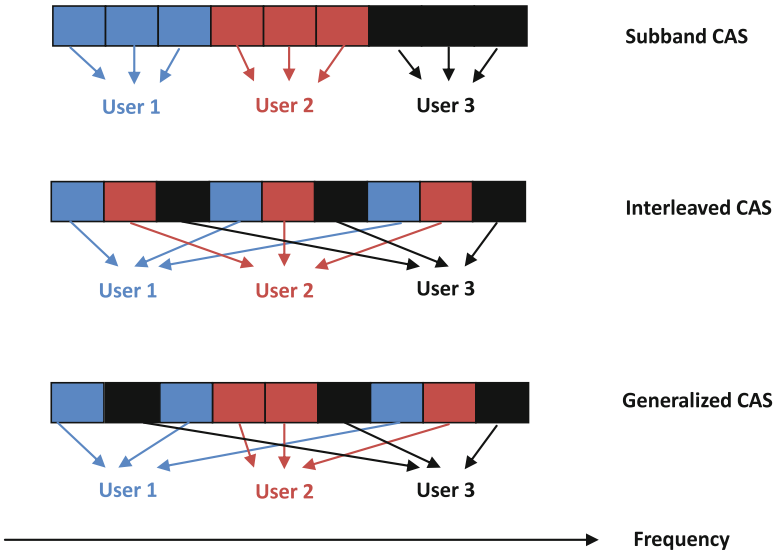

Fig. 2.1 CAS in OFDMA systems

- **Generalized CAS**: individual subcarrier can be assigned to any user, allowing dynamic resource allocation, since no specific rigid relationship between users and subcarriers exists.

Let N and K denote the total number of subcarriers and the number of users, respectively. In OFDMA systems, one subcarrier can be assigned to one user only, and could not be occupied by other users. Assume that all the subcarriers are used for the transmission with no virtual or null subcarrier. Define $\boldsymbol{\Omega}_k(i)$ as the subset of the number of subcarriers allocated to the k-th user ($k = 0, 1, \cdots, K-1$) in the i-th OFDMA block. It can be written as

$$\boldsymbol{\Omega}_k(i) = \{\Omega_k(0, i), \quad \Omega_k(1, i), \quad \cdots, \quad \Omega_k(N-1, i)\}, \tag{2.5}$$

where $\Omega_k(n, i)$ denotes the indicator of subcarrier allocation for the k-th user on the n-th subcarrier in the i-th OFDMA block, given as

$$\Omega_k(n, i) = \begin{cases} 1 \text{ if } \Omega_k(n, i) \text{ occupied by the } k\text{-th user} \\ 0 \text{ if } \Omega_k(n, i) \text{ not occupied by the } k\text{-th user} \end{cases}. \tag{2.6}$$

The union of subsets of subcarriers for K users satisfies

$$\boldsymbol{\Omega}_0(i) \bigcup \boldsymbol{\Omega}_1(i) \cdots \bigcup \boldsymbol{\Omega}_{K-1}(i) = \prod_N = \{N\}, \tag{2.7}$$

The intersection of subsets of subcarriers for K users satisfies

$$\boldsymbol{\Omega}_0(i) \bigcap \boldsymbol{\Omega}_1(i) \cdots \bigcap \boldsymbol{\Omega}_{K-1}(i) = \emptyset, \tag{2.8}$$

where $\emptyset$ denotes an empty set. Let $x_k(n, i)$ denote the symbol on the n-th subcarrier in the i-th block, and transmitted by the k-th user. After subcarrier allocation, the resulting symbol $s_k(n, i)$ in OFDMA systems is given by

$$s_k(n, i) = x_k(n, i) \cdot \Omega_k(n, i). \tag{2.9}$$

The orthogonality between subcarriers provides the intrinsic protection against the Multiple-User Interference (MUI). Therefore, OFDMA inherits from OFDM, the ability to have a simple equalization scheme in the frequency domain. However, there are several technical challenges in OFDMA systems, some of which are frequency and timing synchronisation. Similar to OFDM, OFDMA is extremely sensitive to the CFO and STO [15, 20, 21]. As discussed previously, The CFO destroys the orthogonality between subcarriers and results in the ICI. The STO gives rise to either the ISI or phase shift in the received signals. In particular, multiple users are allowed to transmit simultaneously in OFDMA systems, posing more challenges for multi-CFO and multi-STO estimation. In Chap. 6, a joint algorithm for ICI mitigation and equalization is proposed in the OFDMA uplink.

2.2 MIMO OFDM Systems

To improve system capacity, multiple transmit and receive antennas are employed to establish multiple spatial branches, referred to as MIMO systems [22], as illustrated in Fig. 2.2. Compared to traditional SISO systems, MIMO systems can increase bandwidth efficiency, as multiple transmit and receive antennas operate on the same frequency band for the signal transmission. In order to combat frequency selective fading, OFDM is well suited for use in MIMO systems. Also, equalization can be simplified in the frequency domain for OFDM based systems. Therefore, MIMO OFDM systems have been adopted by the wireless local area networks IEEE 802.11 standards and LTE Advanced, respectively [6–8]. However, as the prorogation path between each transmit antenna and each receive antenna is independent, MIMO OFDM systems give rise to an additional spatial interference, known as the Co-Antenna Interference (CAI) or Co-Channel Interference (CCI) [23], which needs to be eliminated.

An MIMO OFDM system is considered, with K transmit and M receive antennas in the frequency selective fading environment, as illustrated in Fig. 2.4. The incoming serial data at the transmitter is divided into parallels. The IDFT/DFT pair allows

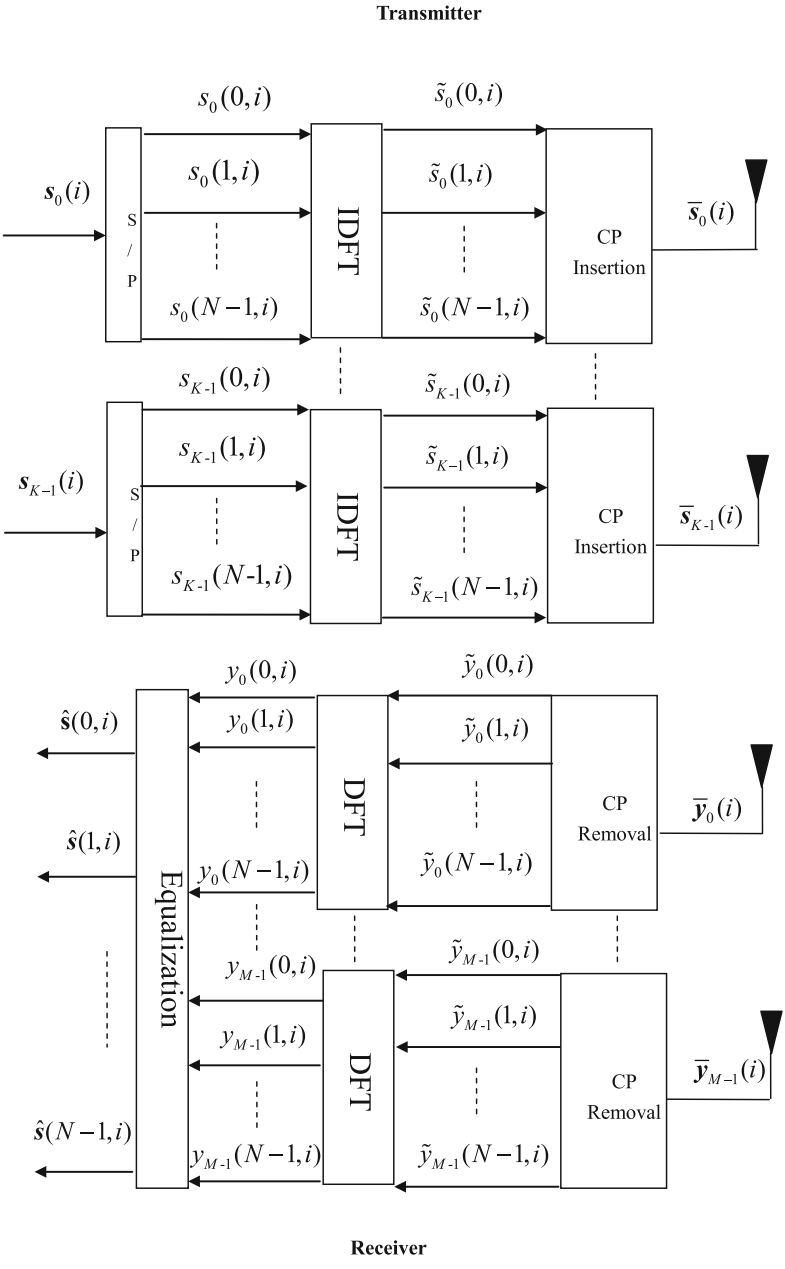

Fig. 2.2 MIMO OFDM systems block diagram

the signal to be transferred in between the frequency domain and the time domain. Let $s_k(n,i)$ denote the symbol on the n-th subcarrier ($n = 0,1,\ldots,N-1$) in the i-th block ($i = 0,1,\ldots,N_s-1$) transmitted by the k-th transmit antenna ($k = 0,1,\ldots,K-1$). Define $\mathbf{s}_k(i) = [s_k(0,i), s_k(1,i)\ldots, s_k(N-1,i)]^T$ as the signal vector in the i-th block for the k-th transmit antenna. Details of the entire process of the data transfer from transmitter to receiver via channels are described in the following steps.

At the transmitter, the signal in the i-th OFDM block is first transformed to the time domain as $\tilde{\mathbf{s}}_k(i)$ by the IDFT as

$$\tilde{\mathbf{s}}_k(i) = \mathbf{F}^H \mathbf{s}_k(i), \tag{2.10}$$

where $\mathbf{F}$ is an $N \times N$ DFT matrix, with the (a,b)-th entry given by $\mathbf{F}(a,b) = \frac{1}{\sqrt{N}} e^{\frac{-j2\pi ab}{N}}$, $(a,b = 0,\ldots,N-1)$, and $\mathbf{F}^H$ is an IDFT matrix, with $\mathbf{F}^H = \mathbf{F}^{-1}$ since $\mathbf{F}$ is a unitary matrix [16]. Note that the computationally efficient IFFT/FFT pair may also be employed.

Assuming a total number of L channel paths, a Cyclic Prefix (CP) of length L_{CP}, at least $L_{\text{CP}} \geq L-1$, is attached to each OFDM block $\tilde{\mathbf{s}}_k(i)$. The guard symbols consist of a copy of the last L_{CP} entries of each OFDM block. The insertion of a CP has two purposes: Inter-Block Interference (IBI) avoidance and circular convolution between time-domain signal and Channel Impulse Response (CIR). With the CP insertion, the transmitted signal vector $\bar{\mathbf{s}}_k(i)$ can be given as

$$\bar{\mathbf{s}}_k(i) = \mathbf{T}_{\text{CP}} \tilde{\mathbf{s}}_k(i), \tag{2.11}$$

where $\mathbf{T}_{\text{CP}} = [\mathbf{I}_{\text{CP}}^T, \mathbf{I}_N^T]^T$ is the $(L_{\text{CP}} + N) \times N$ matrix, with $\mathbf{I}_N$ denoting an $N \times N$ identity matrix and $\mathbf{I}_{\text{CP}}$ denoting the last L_{CP} rows of $\mathbf{I}_N$.

The signal is then transmitted through the frequency selective fading channel, which is assumed to be constant for the duration of a frame consisting of a total number of N_s OFDM blocks. This is a convolution process as shown in Fig. 2.3. The received signal vector $\bar{\mathbf{y}}_m(i) = [\bar{y}_m(0,i), \bar{y}_m(1,i)\ldots, \bar{y}_m(N-1,i)]^T$ at the m-th receive antenna ($m = 0,1,\ldots,M-1$) in the time domain can be written as

$$\bar{\mathbf{y}}_m(i) = \sum_{k=0}^{K-1} \bar{\mathbf{H}}_{m,k} \bar{\mathbf{s}}_k(i) + \bar{\mathbf{z}}_m(i), \tag{2.12}$$

where $\tilde{\mathbf{H}}_{m,k}$ is the $(L_{\text{CP}}+N) \times (L_{\text{CP}}+N)$ convolutional channel matrix between the m-th receive antenna and the k-th transmit antenna, given as

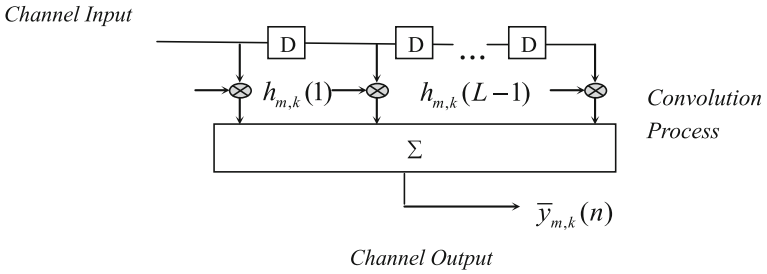

Fig. 2.3 Convolution process of signal and channel for MIMO OFDM systems

$$\bar{\mathbf{H}}_{m,k} = \begin{bmatrix} h_{m,k}(0) & 0 & \cdots & \cdots & 0 \\ \vdots & h_{m,k}(0) & 0 & \cdots & 0 \\ h_{m,k}(L-1) & & \ddots & & \vdots \\ \vdots & \ddots & & \ddots & 0 \\ 0 & \cdots & h_{m,k}(L-1) & \cdots & h_{m,k}(0) \end{bmatrix}, \tag{2.13}$$

where $h_{m,k}(l)$ is the l-th ($l = 0, 1, \ldots, L-1$) channel path between the m-th receive antenna and the k-th transmit antenna, and $\bar{\mathbf{z}}_m(i)$ is the AWGN vector whose entries are Independent Identically Distributed (i.i.d.) complex Gaussian random variables with a zero mean and a variance of N_0 [22].

After the CP is removed, the received signal vector $\tilde{\mathbf{y}}_m(i)$ at the m-th receive antenna can be written as

$$\tilde{\mathbf{y}}_m(i) = \mathbf{R}_{\text{CP}} \bar{\mathbf{y}}_m(i), \tag{2.14}$$

where $\mathbf{R}_{\text{CP}} = [\mathbf{0}_{N \times L_{\text{CP}}}, \mathbf{I}_N]$ is the $N \times (L_{\text{CP}} + N)$ matrix used to remove the CP, with $\mathbf{0}_{N \times L_{\text{CP}}}$ denoting the $N \times L_{\text{CP}}$ matrix filled with zeros.

The received signal is transformed to the frequency domain by applying the $N \times N$ DFT matrix to $\tilde{\mathbf{y}}_m(i)$ as

$$\mathbf{y}_m(i) = \mathbf{F} \tilde{\mathbf{y}}_m(i). \tag{2.15}$$

The full circular convolution process between channel and signal can be achieved using the CP. The time-domain circular convolution can be transformed to a linear multiplication in the frequency domain by applying the IDFT/DFT pair, leading to simple equalization for the frequency selective fading environment [24]. The circulant matrix is a Toeplitz matrix where each row is equal to the previous one rotated by one element [16]. By using the IDFT/DFT pair, the circulant matrix can be diagonalized [16]. The resulting transceiver signal model in the frequency domain can be written as

$$\mathbf{y}_m(i) = \sum_{k=0}^{K-1} \mathbf{H}_{m,k}\mathbf{s}_k(i) + \mathbf{z}_m(i), \tag{2.16}$$

where $\mathbf{H}_{m,k} = \mathbf{F}\tilde{\mathbf{H}}_{m,k}\mathbf{F}^H$ is the diagonal frequency-domain channel matrix, with $\tilde{\mathbf{H}}_{m,k} = \mathbf{R}_{\text{CP}}\bar{\mathbf{H}}_{m,k}\mathbf{T}_{\text{CP}}$ denoting the equivalent circulant channel matrix. The entry (n, n) in $\mathbf{H}_{m,k}$ is written as $H_{m,k}(n, n) = \sum_{l=0}^{L-1} h_{m,k}(l)e^{-\frac{j2\pi nl}{N}}$, and $\mathbf{z}_m(i) = \mathbf{F}\mathbf{R}_{\text{CP}}\bar{\mathbf{z}}_m(i)$ is the frequency-domain noise vector. Note that the distribution statistics of the channel can be preserved by the DFT [22], if the CIR $h_{m,k}(l)$ is assumed to have the Rayleigh distributed magnitude and uniformly distributed phase. Also, the distribution of the white Gaussian noise samples can be preserved by the DFT.

Finally, as the frequency selective fading channel is divided into a number of flat fading channels, Frequency Domain Equalization (FDE) can be performed on each subcarrier to simplify the equalization process for MIMO OFDM systems, Define $\mathbf{s}(n, i) = [s_0(n, i), s_1(n, i), \ldots, s_{K-1}(n, i)]^T$ as the signal vector from K transmit antennas on the n-th subcarrier in the i-th block. The received signal vector $\mathbf{y}(n, i) = [y_0(n, i), y_1(n, i), \ldots, y_{M-1}(n, i)]^T$ in the frequency domain on the n-th subcarrier can be written as

$$\mathbf{y}(n, i) = \mathbf{H}(n)\mathbf{s}(n, i) + \mathbf{z}(n), \tag{2.17}$$

where $\mathbf{H}(n)$ is the $M \times K$ channel frequency response matrix on the n-th subcarrier, with $H_{m,k}(n)$ denoting the entry (m, k) in $\mathbf{H}(n)$, the channel frequency response between the m-th receive antenna and the k-th transmit antenna, and $\mathbf{z}(n)$ is the noise vector. The source data estimate $\hat{\mathbf{s}}(n, i)$ can be performed by either Zero Forcing (ZF) or Minimum Mean Square Error (MMSE) based equalization on the received signal on the n-th subcarrier as

$$\hat{\mathbf{s}}(n, i) = \mathbf{G}(n, i)\mathbf{y}(n, i), \tag{2.18}$$

where $\mathbf{G}(n, i)$ is the weighting matrix that can have either ZF or MMSE equalization criterion. The details of these equalization schemes are provided in the next chapter.

2.3 CoMP Transmission

The inter-cell interference is a major bottleneck for achieving very high data rates in wireless communication systems [23]. Previously, adjacent cells were operated on different frequencies to effectively reduce the inter-cell interference [25]. Recent research trends hint that millimeter (mm) wave communication will be the key component in 5G cellular systems. The short coverage of mm wave bands results in small cells. As the demand for high mobile data rates grows, higher spectral efficiency of cellular networks is needed, with full frequency reuse [26, 27]. One of best ways to manage interference is to allow each BS to connect to each other

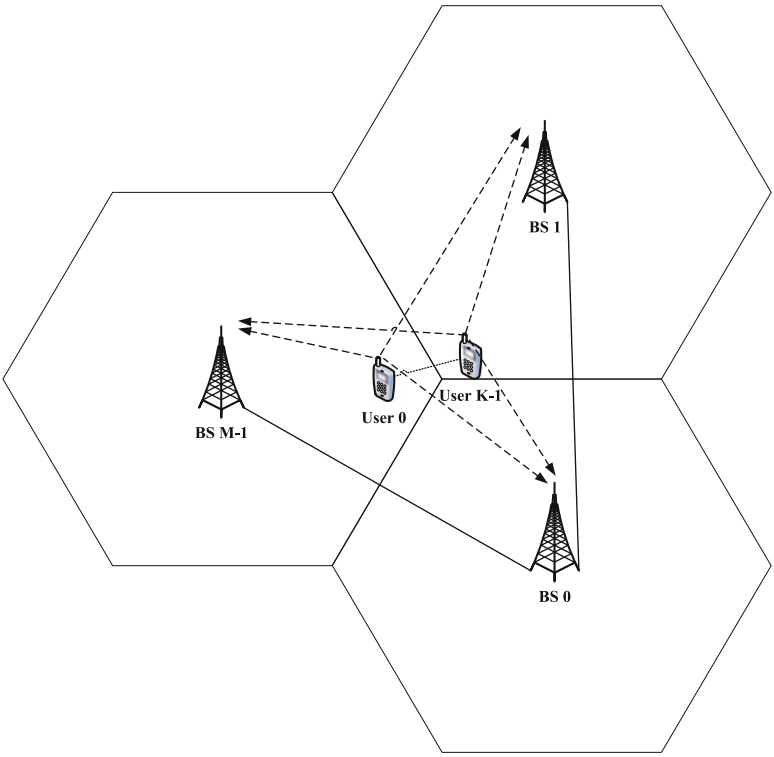

Fig. 2.4 Wireless CoMP system model with K users and M BSs

through a backhaul link. The BSs could exchange messages and jointly process received multiple users' signals on the same frequency band. This structure, called CoMP, has been adopted by LTE-Advanced [28]. CoMP transmission explores the interference between cells, which is different from other existing methods by treating them as noise [29, 30]. These features of CoMP systems are important for users at the cell-edge to have effective communication through the BSs. Also, CoMP is a cost-effective structure, as it requires little change to the current system. The general CoMP system diagram is illustrated in Fig. 2.4.

CoMP transmission has some significant challenges, which are summarized as follows.

- Multi-CFO estimation: As each BS or user has its own oscillator, there are multiple CFOs in the OFDM based CoMP transmission. The multi-CFO estimation becomes much difficult so that conventional frequency synchronization schemes for a single CFO are not suitable in the scenario. Compared to OFDMA systems, multi-CFO estimation in the CoMP transmission is much more challenging. There are two reasons. Firstly, the CoMP system allows users to transmit signals simultaneously by using all shared subcarriers, while multiple users

could not share the same subcarriers in OFDMA systems. In the presence of multiple CFOs, one user's signal power is leaked into other users in OFDMA systems. The effect disappears with correct CFO compensation. By using this property, a number of multi-CFO estimation approaches were proposed for OFDMA systems [20, 31]. However, in the CoMP transmission, different users' signals interfere with each other at different BSs. This interference could not be removed, even in the case of no CFO. These multi-CFO estimation approaches used in OFDMA systems will significantly degrade the performance in the CoMP transmission, and therefore, are not suitable. Secondly, as frequency synchronization of all BSs and users is required, the number of CFOs linearly increases with the increasing number of BSs and users in the CoMP transmission. While in OFDMA systems, the number of CFOs only increases with the number of users. Thus, the number of CFOs in CoMP systems is larger than that in OFDMA systems.

- Multi-cell channel estimation and equalization: On the one hand, the central station in the CoMP transmission requires additional time to collect all received signals from multiple BSs for joint processing. This delay might cause a serious situation in time-limited communications. Thus, low-complexity multi-cell channel estimation and equalization are important and challenging in the CoMP transmission [32]. On the other hand, bandwidth resource is very scarce in wireless communication systems. Traditionally, training signals are commonly used for channel estimation. However, transmitting training signals reduces spectral efficiency. Therefore, there is a trade-off between complexity and spectral efficiency, when designing channel estimation and equalization schemes for the CoMP transmission.

In Chap. 5, a low-complexity multi-CFO estimation method and an ICA based equalization scheme are presented for CoMP systems to well deal with the challenges above.

2.4 CA Technology

CA, as one of key features in LTE-Advanced [28, 33], allows several smaller component carriers (spectrum chunk) to be aggregated. Thus, high data rates can be achieved in the CA transmission, by deploying extended bandwidth for the concurrent transmission. The main purposes for introducing the CA are listed as follows.

- High data rates: Up to five component carriers can be allowed for the aggregation in the both uplink and downlink. As the bandwidth is up to 20 MHz for each component carrier, a maximum of 100 MHz is achieved in the supported bandwidth for five component carriers in total. The peak target data rates are in excess of 1 Gbps in the downlink and 500 Mbps in the uplink, respectively.

- Configuration flexibility: It is possible to have asymmetric configurations for the CA at user and BS. Also, the number of component carriers could be used differently in the downlink and uplink.
- Frequency flexibility: As the locations of users are different, they can select component carriers based on several conditions, such as CSI. This can provide great frequency flexibility. This flexibility also allows for efficient support in power control and component carrier allocation.
- Interference management: the CA can be used as a promising inter-cell interference coordinator, and is dependent on many factors: the relative locations of BSs, traffic situation, the mutual interference coupling and so on. These factors are configured to optimize system performance.

In terms of frequency location, there are three different aggregation scenarios, as shown in Fig. 2.5 [34]. These aggregation scenarios are described as below.

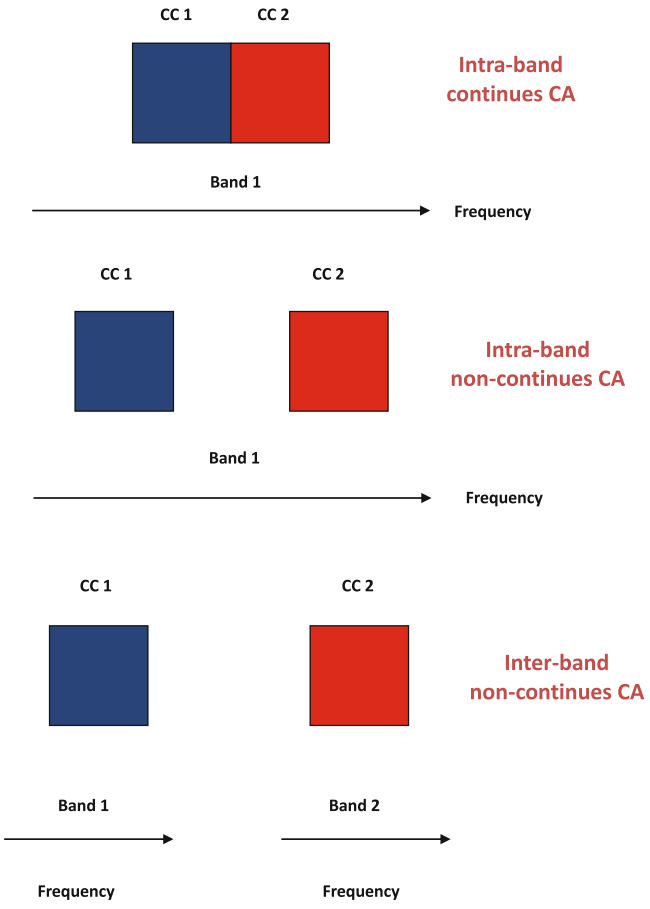

Fig. 2.5 A number of CA types (CC: component carrier)

- Intra-band aggregation with contiguous carriers: A number of continuous component carriers are aggregated within the same bandwidth.
- Intra-band aggregation with non-contiguous carriers: A number of separated component carriers, belonging to the same bandwidth, are aggregated.
- Inter-band aggregation with non-contiguous carriers: A number of non-adjacent component carriers over different bands are aggregated. The exploitation of fragmented spectrums is utilized to enhance frequency flexibility, as the idle bandwidth available can be employed.

For the case of intra-band aggregation with contiguous carriers, only a single transmit chain is used, because the aggregated carriers are contiguous. While there are multiple transmit chains in the non-contiguous carriers. The CA type selection, either contiguous or non-contiguous, depends on the trade-off between cost, complexity and the range of transmission bandwidth. One of targets for LTE-Advanced is expected to provide improvement in cell-edge spectral efficiency [28]. To meet the target, the inter-band non-contiguous CA can be effectively employed in CoMP systems to improve cell-edge throughput, since other idle bandwidths can be combined for the concurrent transmission. However, extra multiple CFOs occur since multiple LOs are used to support the non-continuous carriers on different frequency bands. In Chap. 6, a solution to the multi-CFO problem is proposed for CA based CoMP OFDMA systems by using a semi-blind ICA based joint ICI mitigation and equalization scheme.

References

1. R. Schober. Noncoherent space-time equalization. *IEEE Transactions on Wireless Communications*, 2(3):537–548, May 2003.
2. L. Sarperi, X. Zhu, and A. K. Nandi. Reduced complexity blind layered space-time equalization for MIMO OFDM systems. In *Proc.IEEE International Symposium on Personal Indoor and Mobile Radio Communications (PIMRC)*, Berlin, Germany, Sep. 2005.
3. X. Zhu and R. D. Murch. Layered space-time equalization for wireless MIMO systems. *IEEE Transactions on Wireless Communications*, 2(6):1189–1203, Nov. 2003.
4. S.Weinstein and P. Ebert. Data transmission by frequency-division multiplexing using the discrete fourier transform. *IEEE Transactions on Communications*, 19(5):628–634, Oct. 1971.
5. Z. Wang and G. B. Giannakis. Wireless multicarrier communications. *IEEE Signal Processing Magazine*, 17(3):29–48, May 2000.
6. Ieee standard for information technology-telecommunications and information exchange between systems-local and metropolitan area networks-specific requirements part 11: Wireless lan medium access control (mac) and physical layer (phy) specifications, Mar. 2012.
7. K. Fazel and S. Kaiser. *Multi-carrier and spread spectrum systems: from OFDM and MC-CDMA to LTE and WiMAX*. John Wiley & Sons, New York, USA, second edition, 2008.
8. A. Technologies. *LTE and the Evolution to 4G Wireless: Design and Measurement Challenges*. John Wiley & Sons, New York, USA, 2009.
9. C. J. Hansen. WiGiG: Multi-gigabit wireless communications in the 60 Ghz band. *IEEE Wireless Communications Magazine*, 18(6):6–7, Dec. 2011.
10. Ieee draft standard for local and metropolitan area networks - specific requirements - part 11: Wireless lan medium access control (mac) and physical layer (phy) specifications amendment 3: Enhancements for very high throughput in the 60 ghz band, Jul. 2012.

11. A. Georgakopoulos, D. Karvounas, and K. Tsagkaris. 5G on the horizon: key challenges for the radio-access network. *IEEE Vehicular Technology Magazine*, 8(3):47–53, Jul. 2013.
12. C. Edwards. 5G searches for formula to shake off Shannon. *Engineering & Technology*, 8(8):82–85, Oct. 2013.
13. J. A. C. Bingham. Multi-carrier modulation for data transmission: an idea whose time has come. *IEEE Communications Magazine*, 28(5):17–25, May 1990.
14. P. P. Vaidyanathan. *Multi-Rate System and Filter Banks*. Prentice Hall, 1993.
15. Y. S. Cho, J. Kim, W. Y. Yang, and C. G. Kang. *MIMO-OFDM Wireless Communications with MATLAB*. Wiley, Singapore, 2010.
16. C. D. Meyer. *Matrix Analysis and Applied Linear Algebra*. Society for Industrial and Applied Mathematics, Philadelphia, U.S.A., 2000.
17. Interaction channel for digital terrestrial television (rct) incorporating multiple access ofdm,, Mar. 2001.
18. Ieee standard for local and metropolitan area networks, part 16: Air interface for fixed and mobile broadband wireless access systems amendment2: Physical and medium access control layers for combined fixed and mobile operation in licensed bands, 2005.
19. M. Morelli, C. C. J. Kuo, and M. O. Pun. Synchronization techniques for orthogonal frequency division multiple access (OFDMA): a tutorial review. *Proceedings of the IEEE*, 95(7): 1394–1427, Jul. 2007.
20. M. Movahhedian, Y. Ma, and R. Tafazolli. Blind CFO estimation for linearly precoded OFDMA uplink. *IEEE Transactions on Signal Processing*, 58(9):4698–4710, Sep. 2010.
21. S. Manohar, D. Sreedhar, V. Tikiya, and A. Chockalingam. Cancellation of multiuser interference due to carrier frequency offsets in uplink OFDMA. *IEEE Transactions on Wireless Communications*, 6(7):2560–2571, Jul. 2007.
22. A. J. Paulraj, R. Nabar, and D. Gore. *Introduction to Space-Time Wireless Communications*. Cambridge University Press, Cambridge, U.K., 2003.
23. A. Goldsmith. *Wireless Communications*. Cambridge University Press, London, U.K., 2005.
24. S. J. Orfanidis. *Introduction to Signal Processing*. Prentice Hall, Upper Saddle River, U.S.A., 1996.
25. T.D. Novlan, R. K. Ganti, A. Ghosh, and J. G. Andrews. Analytical evaluation of fractional frequency reuse for OFDMA cellular networks. *IEEE Transactions on Wireless Communications*, 10(12):4294–4305, Dec. 2011.
26. A. Sklavos, T. Weber, E. Costa, H. Haas, and E. Schulz. Joint detection in multi-antenna and multi-user OFDM systems. *Multi-Carrier Spread Spectrum and Related Topics*, pages 191–198, May 2002.
27. S. Shamai, O. Somekh, and B. Zaidel. Multi-cell communications: a new look at interference. *IEEE Journal on Selected Areas in Communications*, 28(9):1380–1408, Dec. 2010.
28. 3gpp technical report 36.814 version 9.0.0, further advancements for e-utra physical layer aspects, Mar. 2010.
29. J. Andrews. Interference cancellation for cellular systems: a contemporary overview. *IEEE Transaction on Wireless Communications*, 12(2):19–29, Apr. 2005.
30. P. Marsch, S. Khattak, and G. Fettweis. A framework for determining realistic capacity bounds for distributed antenna systems. In *Proc. IEEE Information Theory Workshop*, pages 571–575, Chengdu, China, Oct. 2006.
31. P. Sun and L. Zhang. Low complexity pilot aided frequency synchronization for OFDMA uplink transmission. *IEEE Transaction on Wireless Communications*, 8(7):3758–3769, Jul. 2009.
32. J. Hoydis, M. Kobayashi, and M. Debbah. Optimal channel training in uplink network MIMO systems. *IEEE Transactions on Signal Processing*, 59(6):2824–2834, 2011.
33. Z. Shen, A. Papasakellariou, J. Montojo, D. Gerstenberger, and F. Xu. Overview of 3GPP LTE-Advanced carrier aggregation for 4G wireless communications. *IEEE Communications Magazine*, 50(2):122–130, Feb. 2012.
34. K. I. Pedersen, F. Frederiksen, C. Rosa, L. G. U. Garcia H. Nguyen, and Y. Wang. Carrier aggregation for LTE Advanced: functionality and performance aspects. *IEEE Communications Magazine*, 49(6):89–95, Jun. 2011.

http://www.springer.com/978-3-319-24984-1

Semi-Blind Carrier Frequency Offset Estimation and Channel Equalization

Jiang, Y.; Zhu, X.; Lim, E.G.; Huang, Y.; Lin, H.

2015, X, 87 p. 17 illus., 6 illus. in color.,
ISBN: 978-3-319-24984-1